PAPER

Check for updates

Quaternary ammonium surfmers: synthesis, characterization and antibacterial performance

Cailing Li, Jinlu Zhong, Yanan Weng, Sensen Xie, Shuang Li and Dinghua Yu (iD) *

Quaternary ammonium surfmers not only possess antibacterial activity, but also provide new active monomers for the synthesis of polymer cationic surfactants. In this study, four quaternary ammonium surfmers (nQAS) were synthesized through the quaternization of dimethylaminoethyl acrylate and brominated alkanes with different carbon chain lengths (n). Their structures were confirmed by ^{1}H nuclear magnetic resonance spectroscopy and high-resolution mass spectrometry. Their surface activities, including surface tension curves, were measured, and the micellar microenvironment of the QASs in pure water and solutions containing electrolytes was studied. With *Staphylococcus aureus* (*S. aureus*) and *Escherichia coli* (*E. coli*) as representatives of Gram-positive and Gram-negative bacteria, respectively, the minimal inhibition concentration (MIC) and minimum bactericidal concentration (MBC) were investigated by the classical plate counting method. The 18QAS surfmer showed a very low MIC and MBC of 0.937 and 3.75 μmol L^{-1}, respectively, against *S. aureus*, with a killing efficiency of 4.23 log CFU, and 16QAS showed a superior killing efficiency of 2.61 log CFU against *E. coli* at a concentration of 32.25 μmol L^{-1}. These quaternary ammonium surfmers could provide functional monomers for long-term antibacterial surface coating and other biological applications.

1. Introduction

The surfaces of solid materials, such as medical equipment, devices, and environmental surfaces, play a very important role in the transmission of pathogenic microorganisms. In clinical practice, if reused medical devices are not properly cleaned and sterilized, residual bacteria and biofilms can not only cause corrosion of the devices, but also easily lead to surgical infections. Meanwhile, interventional therapy has become a commonly used surgical treatment method in clinical practice, and implant biomaterials are prone to contamination by bacteria or biofilms due to their strong adsorption characteristics. Therefore, the antibacterial design of the surface of such materials is a hot topic in the field of medical device research.[1] According to antibacterial mechanisms, current antibacterial strategies for biomaterials can be categorized into passive or active protocols. Passive antibacterial surfaces utilize micro-/nanostructured topographies to inhibit bacterial adhesion and colonization.[2] In contrast, active antibacterial strategies can be achieved through the release of antibacterial agents or using a contact-killing surface. Especially, contact-killing surfaces can achieve sustained antibacterial effects through delicate surface-bound amphiphilic chemistries. For decades, cationic surfactants,

with amines or tetraalkylammonium as functional groups, were employed as disinfectants, antiseptics, preservative agents, bactericides and antistatic agents due to their well-known antimicrobial activity and corrosion-inhibiting properties.[3,4] Generally, these cationic surfactants accomplish their antibacterial function through three mechanisms: bacterial membrane disruption *via* electrostatic interactions between surface cationic groups and the negative bacterial surface,[5] insertion of hydrophobic alkyl chains into the lipid envelop,[6] and zwitterionic interface designs.[7] In order to decrease the cytotoxicity of cationic surfactants to mammalian cells, researchers have explored various effective approaches, including the modulation of host–guest supramolecular conformation,[8] the use of cyclodextrin/cationic trimeric surfactant complexes,[9] and the non-covalent assembly of plant gallic acid and quaternary ammonium surfactants.[10] These new methods have effectively prolonged the bactericidal effect of cationic surfactants to a certain extent. Moreover, in order to obtain a long-lasting contact-killing surface, these cationic surfactants can be derivatized to achieve reactive properties, which then allow them to be attached to the surface of materials through chemical bonds. In summary, these polymerizable amphiphilic substances are key materials for achieving sustained antibacterial functions.

Polymerizable surfactants include surface active monomers (surfmers) that have a polymerizable fragment that can be incorporated into polymeric materials. Surfmers

College of Biotechnology and Pharmaceutical Engineering, Nanjing Tech University, Nanjing 211816, PR China. E-mail: yudh@njtech.edu.cn; Tel: +86 25 58139386

are amphiphilic compounds consisting of a polymerizable group (usually hydrophobic) and a hydrophilic head group (neutral or charged), with the head group being a functional group that is referred to as the functional surfmer.[11] Many studies have shown that the length of the hydrophobic chain of the cationic surfactant greatly affects its antimicrobial activity.[12–14] In the synthesis of polymerizable surfactants, both the choice of reactive functional group and the grafting position affect the interfacial properties of the product molecules. Gao et al. introduced an acrylamide group to the branched position of alkyl sulfonic acid. The experimental results showed that branched polymerizable surfactants have characteristic micellar behaviors, including increased solubility, decreased surface adsorption amounts, and improved critical micellar concentrations compared with common anionic surfactants with the same hydrocarbon chain and anionic head group.[15]

Raffaella Mancuso prepared four types of reactive quaternary ammonium surfactants and tested their antimicrobial activity. The results showed that reactive surfactants bearing an alkyl chain of 11 and particularly 12 carbon atoms possessed significant activity against Gram positive bacteria and yeast strains, and revealed that the antibacterial activity was higher than that of dodecyltrimethylammonium bromide with the same carbon chain length.[16] In addition to the position, the type of reactive group also has a significant impact on the properties of the products. For example, ester and amide bonds often appear as connecting groups in the product structures, which will also have a significant impact on the surface and interface properties of the products. Garcia et al. reported that the insertion of a functional amide group into a surfactant side chain generates significant changes in the surface activity and micellization.[17] Hoque et al. studied the solution assembly and interface aggregation behavior of gemini surfactants with and without an amide group, and the results showed that amide functionality increased the surfactant aggregation tendencies compared to the surfactants with no amide bond.[18] In summary, the surfmer composition and molecular structure not only play an extremely important role in the synthesis, but also essentially determine the final surface properties of the functional coatings. Research on surface active monomers is an interdisciplinary field involving physics, chemistry, biology and materials science, and surfmers with novel structures can serve in a wide range of applications, including medicine, pharmacy, and biology.[19]

Reactive quaternary ammonium salts can be polymerized or copolymerized to obtain surfaces with long-lasting contact-killing function. However, it is important to note that the chain length, grafting position, and functional groups of reactive quaternary ammonium salts impact their solution assembly and interface behavior, as well as their bactericidal performance. In this work, four polymerizable quaternary ammonium surfmers with different hydrophobic chain lengths were synthesized with dimethylaminoethyl acrylate

and bromoalkane as raw materials through a quaternization process. The structures of the as-prepared surfmers were confirmed through spectroscopic methods, and the effects of the hydrophobic chain length and the electrolyte on the surface activity and micellar environment of the surfmers were studied. Lastly, with *Staphylococcus aureus* and *Escherichia coli* as representative strains, the bactericidal and inhibitory efficiencies of four polymerizable quaternary ammonium surfmers were compared to those of the control, cetyltrimethylammonium bromide (CTAB). These results provide a good material basis for the construction of long-lasting antibacterial surfaces.

2. Materials and methods

2.1 Materials

Dimethylaminoethyl acrylate (DMAEA), 1-bromododecane (C_{12}–Br), 1-bromotetradecane (C_{14}–Br), 1-bromohexadecane (C_{16}–Br), 1-bromooctadecane (C_{18}–Br), cetyltrimethylammonium bromide (CTAB), tetrahydrofuran and methyl orange (MO) were purchased from Shanghai Aladdin Reagent Co., Ltd. Methanol, methylene chloride, ethyl acetate and petroleum ether were purchased from Wuxi Yasheng Chemical Co., Ltd. The bacterial medium was purchased from Shanghai Shenggong Biotechnology Co., Ltd. All chemicals were supplied in analytical purity and used directly without purification. All standard solutions and samples were prepared using ultra-pure water (resistance 18.2 $M\Omega$ cm^{-1}), purified by the laboratory water purification system (Nanjing Yiou Yida). The bacterial strains, *E. coli* (CCTCC No.: 23429) and *S. aureus* (CICC No.: 21600), used in this study were the same as those reported previously.[20]

2.2 Methods

2.2.1 Preparation of polymerizable quaternary ammonium surfmers. Four polymerizable quaternary ammonium surfmers were synthesized through the quaternization process reported by Chen et al.[21] with minor changes; the synthesis is shown in Fig. 1. C_{12}–Br, C_{14}–Br, C_{16}–Br and C_{18}–Br were used as raw materials to react with DMAEA, and several polymerizable quaternary ammonium surfmers with different hydrophobic chain lengths were obtained. In a typical procedure, 1-bromododecane (0.02 mol), DMAEA (0.01 mol) and tetrahydrofuran (10 mL) were added to a 50 mL three-necked flask equipped with a condenser, a thermometer and a mechanical stirrer, and the mixture was stirred for 24 h at 60 °C. The progress of the reaction was monitored by thin-layer chromatography until DMAEA was consumed. After the reaction, the solvent was removed with
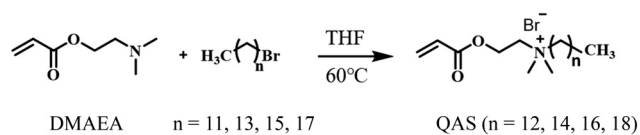

Fig. 1 Synthesis of the four polymerizable quaternary ammonium surfmers.

a rotary evaporator. The unreacted brominated alkanes were washed three times with a mixed solvent of ethyl acetate and petroleum ether (5 : 1), and the acquired product was labeled as 12QAS. Similarly, 14QAS, 16QAS and 18QAS were prepared by the same method.

2.2.2 Characterization methods. ^{1}H NMR spectra were recorded with an AvanceNEO400 nuclear magnetic resonance spectrometer (Bruker, Germany), operating at 400 MHz with deuterated chloroform as solvent.

High-resolution mass spectra (HRMS) were acquired with a Bruker Autoflexmax MALDI-TOF instrument, with electric spray ionization in positive ion mode (ESI$^+$).

2.2.3 Surface tension. The platinum ring method (duNouyRing method)[22] was employed to measure the surface tension curves of the four polymerizable quaternary ammonium surfmers (12QAS, 14QAS, 16QAS, 18QAS) at room temperature using an automatic interfacial tensiometer (BZY-100, Shanghai Fangrui Instrument Co., Ltd.). Before the experiment, the automatic surface tensiometer was calibrated with pure water (surface tension 72.2 mN m^{-1}). Before each measurement, the platinum rings were cleaned with pure water and burned until red with an alcohol lamp to remove possible organic residues. The surface tension was measured in triplicate and the average was taken. For each surfactant, the surface tension value (γ) and its corresponding concentration (C) were plotted as a $\gamma - \ln C$ curve. Their thermodynamic parameters, such as minimum surface tension, critical micelle concentration (CMC), minimum molecular cross-sectional area (A_{min}) and maximum surface excess concentration (Γ), were calculated from the surface tension curves. The surface tension curve of hexadecyl trimethyl ammonium bromide (CTAB) solution was used as a control to analyze the influence of hydrophobic groups on the aggregation behavior of surfactants in water.

In order to analyze the effect of electrolyte on the aggregation behavior of surfactants, 16QAS surfmers were selected and dissolved in deionized water and NaCl solutions at 0.05 M, 0.1 M and 0.2 M. To further study the effects of cation and anion valences, 16QAS surfmers were dissolved in 0.05 mol L^{-1} solutions of NaCl, MgCl$_2$, FeCl$_3$, and Na$_2$SO$_4$ and Na$_3$PO$_4$. The surface tension curves were measured at room temperature using the platinum ring method with an automatic surface tensiometer.

2.2.4 Microenvironment characterization. Methyl orange (MO) can be used as a probe molecule to explore changes in the microenvironment after surfactant assembly.[23] For each surfactant studied, the ultraviolet-visible absorption spectra of different concentrations of surfactant and methyl orange were recorded using a UH5300 ultraviolet-visible spectrophotometer (Hitachi, Japan) equipped with a quartz cell. The final concentration of the MO solution was 50 μmol L^{-1} in different concentrations of surfactant solution. The UV absorption spectra were recorded at a scanning rate of 400 nm min^{-1}, in the wavelength range of 330–580 nm.

2.2.5 In vitro antibacterial activity. According to our previous report,[24] Gram-positive *Staphylococcus aureus* and Gram-negative *Escherichia coli* were used as model strains *in vitro*. Both strains were inoculated into LB broth medium and cultured at 37 °C with shaking at a speed of 200 rpm. After 12 hours, the bacterial concentrations of *E. coli* and *S. aureus* were approximately 10^9 CFU mL^{-1} and 10^8 CFU mL^{-1}, respectively.

To ensure sufficient absorption of QAS surfmers by bacteria, 100 μL of the appropriate concentration of bacterial solution was mixed with 5 μM QAS solution in a sterile centrifuge tube at an equal volume, and incubated for 30 minutes under dark conditions at 37 °C and 300 rpm. Then, 100 μL of the mixed solution was taken and evenly spread on LB broth agar medium. Finally, the plate was transferred to an incubator at 37 °C for 24 hours. After serial dilution in PBS, cell viability was evaluated by counting colony-forming units (CFUs) on agar plates. With PBS as the blank control, the same process was performed to evaluate the antibacterial effect of the QAS surfmers. The above operations were carried out on an ultra-clean workbench, and each test was repeated three times.

2.2.6 Minimum inhibitory concentration (MIC). The minimum inhibitory concentration determination of the as-prepared QAS surfmers was performed using the two-fold microdilution broth method, according to the operating procedures recommended by the Clinical and Laboratory Standards Institute (CLSI) in the United States (CLSI-M07-A8). The antibacterial effects of the QAS surfmers were recorded by monitoring the visible growth of microorganisms in meat broth.[25] For the MIC determination of the QAS surfmers, the bacterial concentration was set at 10^6 CFU mL^{-1}.

Surfmer stock solutions of 1 mM were prepared and diluted by the double dilution method to obtain solutions with concentrations of 0.5 mM, 0.25 mM, 0.125 mM, 0.0625 mM, 0.03125 mM, and 0.015 mM, *etc.*, for future use. Bacterial solution (100 μL) was added to 10 mL of surfmer solution with different concentrations, and mixed thoroughly. With bacterial solutions without surfmer as a control group, three parallel antibacterial measurements were performed for each surfmer concentration. Finally, the samples were placed in an incubator at 37 °C for 12 hours and their turbidities were recorded. The MIC of each surfmer corresponds to the lowest concentration at which visible growth was inhibited. Sub-MIC values are concentrations below the MIC.

2.2.7 Minimum bactericidal concentration (MBC). Based on the MIC results, 100 μL of surfmer solutions with different concentrations (such as 1, 2, 4, and 8 times the MIC) were coated on a solid LB plate and incubated at 37 °C for 24 h. The minimum bactericidal concentration (MBC) of QAS was recorded as the concentration of the antibacterial agent in the medium required to reduce the colony growth number of the incubated bacteria to less than 0.1%.

3. Results and discussion

3.1 Synthesis and structural characterization

In order to construct polymerizable cationic amphiphilic surfmers, dimethylaminoethyl acrylate was used as the

functional reactant. As we know, the structure and the length of the hydrocarbon chain of the surfactant's hydrophobic tail have a significant impact on the interfacial and application properties of surfactants. In order to establish the effect of the hydrophobic tail length of the cationic reactive surfactants on interfacial properties and antibacterial performance, we selected brominated alkanes with different chain lengths to construct the hydrophobic tails of the surfactants. As illustrated in Fig. 1, with several brominated alkanes as the alkylating agents, dimethylaminoethyl acrylate was transformed into a series of polymerizable quaternary ammonium surfmer (QAS) compounds through the quaternization process. In order to confirm the structures of the products, ^{1}H nuclear magnetic resonance spectroscopy (^{1}H NMR) and high-resolution mass spectrometry (HRMS) techniques were used to study the synthesized compounds, and the corresponding results are shown in Fig. 2 and 3.

The ^{1}H NMR spectra of the four polymerizable cationic surfmers are shown in Fig. 2, with the corresponding peaks ascribed to the labeled hydrogen atoms based on the study by Nie et al.[26] and general ^{1}H NMR spectra analysis protocols. As shown in Fig. 1, the structural differences between the four cationic surfmers lie in the different number of carbon atoms in the hydrophobic chain. Thus, their ^{1}H NMR spectra are similar, and the obvious difference should be found at

the characteristic location corresponding to the hydrogen atoms of the methylene groups. The peaks at 0.8–0.9 ppm are typical of hydrogen atoms of methyl ($-CH_3$) groups. The multiple peaks from 1.3–1.4 ppm are ascribed to the typical hydrogen atoms in the methylene groups of the C_{12}–C_{18} hydrocarbon chains in the four QAS surfmers. The peaks at 3.6 and 1.7 ppm could be indexed to the hydrogen atoms on the two methylene groups directly connected to the N atoms. The peaks at 3.5 ppm stem from the hydrogen atoms of the two methyl groups ($-CH_3$) connected to the quaternary ammonium nitrogen. The peaks at 4.2 ppm could be ascribed to the hydrogen atoms in the methylene groups directly connected to the N atoms in the N,N-dimethyl aminoethyl fragments, and the hydrogen atoms in the methylene groups connected to oxygen atoms in the N,N-dimethyl aminoethyl fragments contribute to the peaks at 4.7 ppm. The peaks from 5.9 to 6.5 ppm are attributed to the hydrogen atoms located in the unsaturated carbon chemical environment in the acrylate alkene (CH_2=$CH-$) groups. In summary, comparing the ^{1}H NMR spectra of the four products, as shown in Fig. 2, the number of hydrogen atoms in the methylene group of the different hydrophobic chain lengths is significantly different. According to the peak area integrals, the number of hydrogen atoms is consistent with the theoretical value. Moreover, the presence of hydrogen
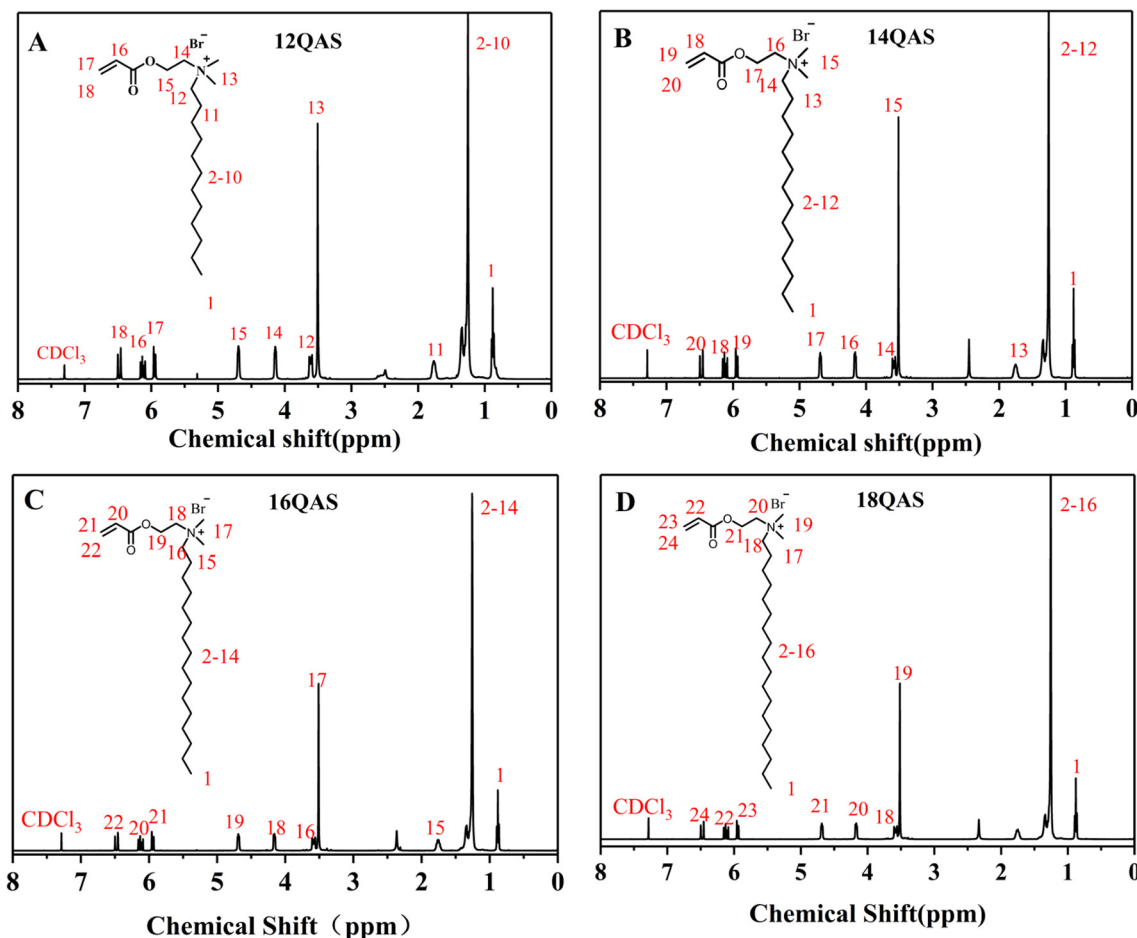

Fig. 2 ^{1}H NMR spectra of the four reactive QAS. (A) 12QAS, (B) 14QAS, (C) 16QAS and (D) 18QAS.
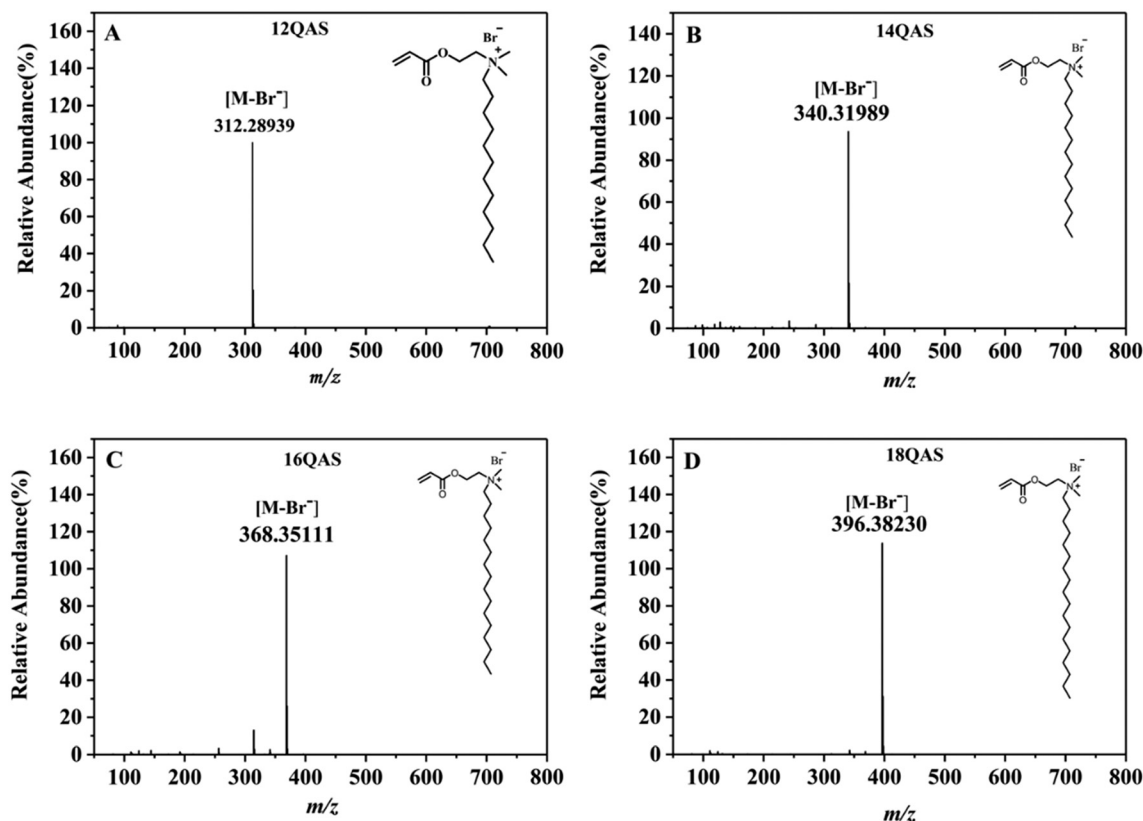
Fig. 3   The mass spectra of the four reactive QASs. (A) 12QAS, (B) 14QAS, (C) 16QAS and (D) 18QAS.

atoms on the unsaturated carbon centers proves that the acrylate polymerizable groups are preserved. The above results indicate that the four polymerizable cation surfmers were successfully synthesized through the synthesis route shown in Fig. 1.

The specific ^{1}H NMR data for the four compounds are as follows:

12QAS. ^{1}H NMR (400 MHz, chloroform-d) δ 6.48 (d, J = 17.3 Hz, 1H), 6.13 (dd, J = 17.2, 10.5 Hz, 1H), 5.95 (d, J = 10.5 Hz, 1H), 4.76–4.61 (m, 2H), 4.22–4.10 (m, 2H), 3.66–3.56 (m, 2H), 3.51 (s, 6H), 1.87–1.71 (m, 2H), 1.41–1.18 (m, 18H), 0.88 (t, J = 6.7 Hz, 3H).

14QAS. ^{1}H NMR (400 MHz, chloroform-d) δ 6.48 (dd, J = 17.3, 1.2 Hz, 1H), 6.12 (dd, J = 17.3, 10.5 Hz, 1H), 5.94 (dd, J = 10.5, 1.2 Hz, 1H), 4.76–4.63 (m, 2H), 4.22–4.11 (m, 2H), 3.65–3.56 (m, 2H), 3.51 (s, 6H), 1.82–1.70 (m, 2H), 1.42–1.19 (m, 20H), 0.88 (t, J = 6.8 Hz, 3H).

16QAS. ^{1}H NMR (400 MHz, chloroform-d) δ 6.53–6.43 (m, 1H), 6.12 (dd, J = 17.3, 10.5 Hz, 1H), 5.98–5.91 (m, 1H), 4.73–4.65 (m, 2H), 4.20–4.12 (m, 2H), 3.63–3.50 (m, 2H), 3.51 (s, 6H), 1.82–1.69 (m, 2H), 1.39–1.20 (m, 22H), 0.88 (t, J = 6.7 Hz, 3H).

18QAS. ^{1}H NMR (400 MHz, chloroform-d) δ 6.48 (dd, J = 17.3, 1.2 Hz, 1H), 6.12 (dd, J = 17.3, 10.4 Hz, 1H), 5.95 (dd, J = 10.4, 1.1 Hz, 1H), 4.72–4.65 (m, 2H), 4.21–4.13 (m, 2H), 3.63–3.50 (m, 2H), 3.52 (s, 6H), 1.82–1.68 (m, 2H), 1.39–1.17 (m, 24H), 0.88 (t, J = 6.7 Hz, 3H).

The four as-synthesized polymerizable cationic surfmers were also analyzed by high-resolution mass spectroscopy, and the corresponding results are shown in Fig. 3. Given that the bromine atoms do not show signals in the mass spectrum, the HRMS results demonstrate the $C_nH_{2n}O_2N^+$ fragments of the four polymerizable cationic surfmers. From Fig. 3, the signals at m/z 312.28939, 340.31989, 368.35111 and 396.38230 correspond to the molecular ion peaks of the four polymerizable cationic surfmers. Thus, the HRMS results shown in Fig. 3 further confirm that the four polymerizable cationic surfmers were successfully synthesized.

3.2 Physical and chemical characterization

3.2.1 Surface tension curves. In order to compare the effects of the structure of the polymerizable quaternary ammonium surfmers on surface tension, hexadecyl trimethyl ammonium bromide (CTAB), with a similar amphiphilic quaternary ammonium structure, was used as a control compound. While the hydrophilic quaternary ammonium is located at the end of CTAB molecules, the as-synthesized polymerizable quaternary ammonium surfmers have the hydrophilic quaternary ammonium located within the molecule, as shown in Fig. 1. Using pure water as the medium, the air-water surface tension curves of the four polymerizable quaternary ammonium surfmers were studied, and the results are shown in Fig. 4.
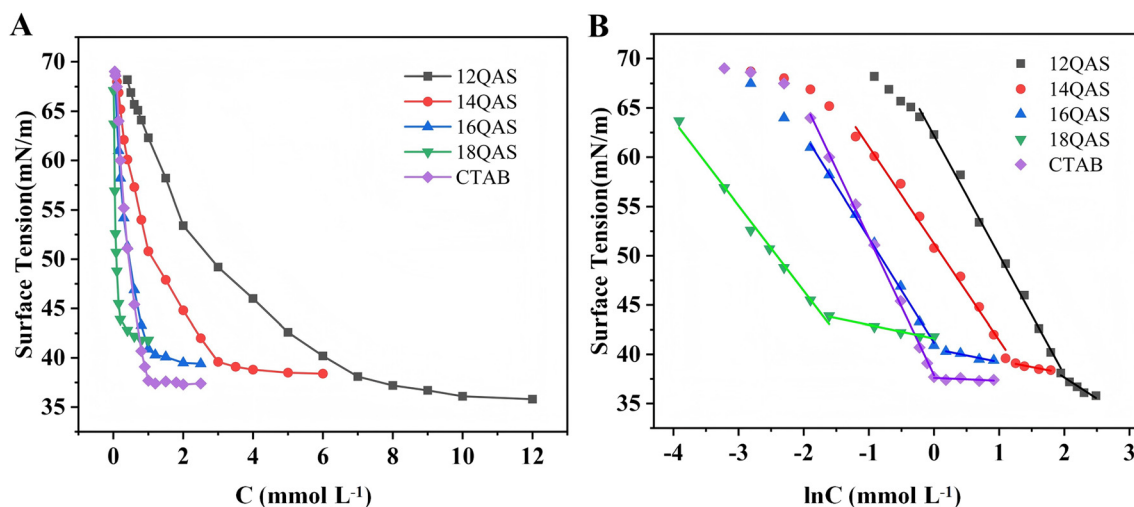
Fig. 4 The surface tension curves of polymerizable quaternary ammonium surfmers (12QAS, 14QAS, 16QAS and 18QAS) and the control CTAB. (A) The surface tension curve. (B) Fitted surface tension ln C results corresponding to surface tension curves.

As shown in Fig. 4(A), with increased concentration, the surface tension of the five amphiphilic quaternary ammonium salts first decreased rapidly and then stabilized, which are typical characteristics of surfactants. Generally, the rapid reduction in the surface tension could be induced by an increase in the packing at the air-water interface of the surfactant molecules with increasing concentration due to their amphiphilic characteristics. Specifically, 12QAS reduced the surface tension of pure water from 72 mN m^{-1} to 36.2 mN m^{-1} (the minimum surface tension), and 14QAS, 16QAS and 18QAS reduced the surface tension of pure water to 38.1 mN m^{-1}, 39.4 mN m^{-1}, and 41.8 mN m^{-1}, respectively. On the other hand, comparing the surface tension curves of the surfmers with different carbon chain lengths, it can be found that the decay rate of surface tension accelerates as the hydrophobic chain length increases, indicating the enhanced surface activity. In order to analyze the surface tension curve more accurately, logarithmic processing was performed on the surface tension curves in Fig. 4(A); the corresponding results are shown in Fig. 4(B). Specifically, two significant features can be observed from Fig. 4(B): the first is the negative slope of the rapidly decreasing part increases with increasing carbon chain length. According to Márquez-Beltrán's theory,[27] the slope of the surface tension curve can be associated with the ability of surfactants to reduce the surface tension of water. These results further confirm that the surface activity of the four polymerizable surfmers increases with increasing carbon chain length. The second phenomenon is the change law of surface tension in low concentration ranges. 12QAS, 14QAS and CTAB all show slow decline tendencies of surface tension in the low concentration range, while 16QAS, 18QAS show a rapid decrease in surface tension. The relationship between surface tension and surfactant concentration reflects the aggregate states of amphiphilic molecules. Micellization is a multistep process, which includes the assembly of surfactant monomers into dimers and trimers, *etc.*[28]

3.2.2 Thermodynamic parameters. According to the classical Gibbs adsorption isotherm equation,[27] a series of thermodynamic parameters such as the critical micelle concentration (CMC), the surface tension at the CMC (γ_{cmc}), the maximum surface excess concentration (Γ_{max}) and the minimum molecular cross-sectional area (A_{min}) of different surfactants at the air–water interface are calculated. The formula is as follows:

$$\Gamma = -1/nRT[\partial\sigma/\partial\ln(C_s)]$$

$$A = 1/(\Gamma \times NA)$$

In the above equation, σ represents the surface tension in mN m^{-1}, R is the gas constant with a value of 8.31 J mol^{-1} K^{-1}, and T is the absolute temperature in Kelvin. C_s represents the concentration of the surfactant in mol L^{-1}, while n is a constant that depends on the amount of substance adsorbed by the surfactant at the interface (according to previous reports, $n = 2$).[29] Finally, NA represents Avogadro's constant (6.02×10^{23} mol^{-1}).

According to surface tension $-\ln C$ curves in Fig. 4(B), the critical micelle concentration and the minimum surface tension of the five quaternary ammonium surfactants were calculated; the corresponding results are listed in Table 1. The CMC of 12QAS was determined to be 7.19 mmol L^{-1}. Meanwhile, 14QAS, 16QAS, and 18QAS had lower CMC values

Table 1 Adsorption parameters of polymerizable quaternary ammonium surfmers with different carbon chain lengths and CTAB at 298 K

Samples	γ_{cmc}	CMC (mmol L^{-1})	Γ (μmol m^{-2})	A_{min} (Å^2)	PC$_{20}$
12QAS	36.2	7.19	2.30	72.22	−0.840
14QAS	38.1	3.27	2.19	75.85	0.077
16QAS	39.4	1.05	2.14	77.48	1.019
18QAS	41.8	0.18	1.75	95.08	2.643
CTAB	37.4	1.02	2.82	58.99	1.013

of 3.27 mmol L^{-1}, 1.05 mmol L^{-1}, and 0.18 mmol L^{-1}, respectively. These results demonstrate that the CMC of the four polymerizable quaternary ammonium surfmers gradually decreases with increasing chain length of the hydrophobic tails. The decrease in the CMC with an increasing hydrophobic chain length can be explained by the increased ability of the molecules to migrate to the surface to form micelles at low concentrations.[30] Compared with 12QAS, the 14QAS, 16QAS, and 18QAS surfactants have a higher tendency to migrate to the air/water interface. It is worth noting that the CMC values of CTAB and 16QAS are not much different, because they have the same number of carbon atoms.

The corresponding adsorption parameters of the five polymerizable quaternary ammonium surfactants, including surface excess concentration (Γ) and cross-sectional area (A), were also calculated according to the above equation; the results are listed in Table 1. Obviously, A_{min} is related to the Γ_{max} value. The four polymerizable quaternary ammonium surfmers showed larger minimum molecular cross-sectional areas (72.22, 75.85, 77.48 and 95.08 Å^2, respectively) than CTAB (58.99 Å^2). The larger occupied area results indicate that the branched structures of the acrylate polymerizable hydrophobic group induce a larger occupied molecular area when packing at the air–water interface.

In addition, the surfactant efficiency of decreasing surface tension refers to the concentration required to achieve a given surface tension; lower concentrations imply higher efficiencies. Generally, it is expressed as the negative logarithm pC$_{20}$ of the concentration required to reduce the surface tension by 20 mN m^{-1} as follows:

$$pC_{20} = -lgC_{20}$$

According to the above equation, the pC$_{20}$ values for 12QAS, 14QAS, 16QAS, 18QAS and CTAB were calculated based on the surface tension curves shown in Fig. 4; the results are listed in Table 1. The corresponding pC$_{20}$ values for 12QAS, 14QAS, 16QAS, and 18QAS are −0.84, 0.077, 1.019 and 2.643, respectively. When the hydrophobic chain length increases, the corresponding pC$_{20}$ value gradually increases, indicating that the efficiency with which the surfmer can reduce the surface tension increases with increasing hydrophobic chain length.

3.2.3 Effect of electrolytes on surfactants. The synergistic effect of electrolytes and surfactants has always been a hot topic in scientific research and industrial applications. When ionic surfactants are dissolved in water, they are ionized to form cations and anions. Therefore, the type and concentration of electrolytes present in the solution will greatly affect microprocesses such as interfacial adsorption, micelle formation, and dissociation of surfactants.[31] In many applications, salts are present or added as an extra additive to enhance the performance of surfactants. Salts can significantly affect the equilibrium surfactant behavior by changing the critical micellar concentrations (CMC),
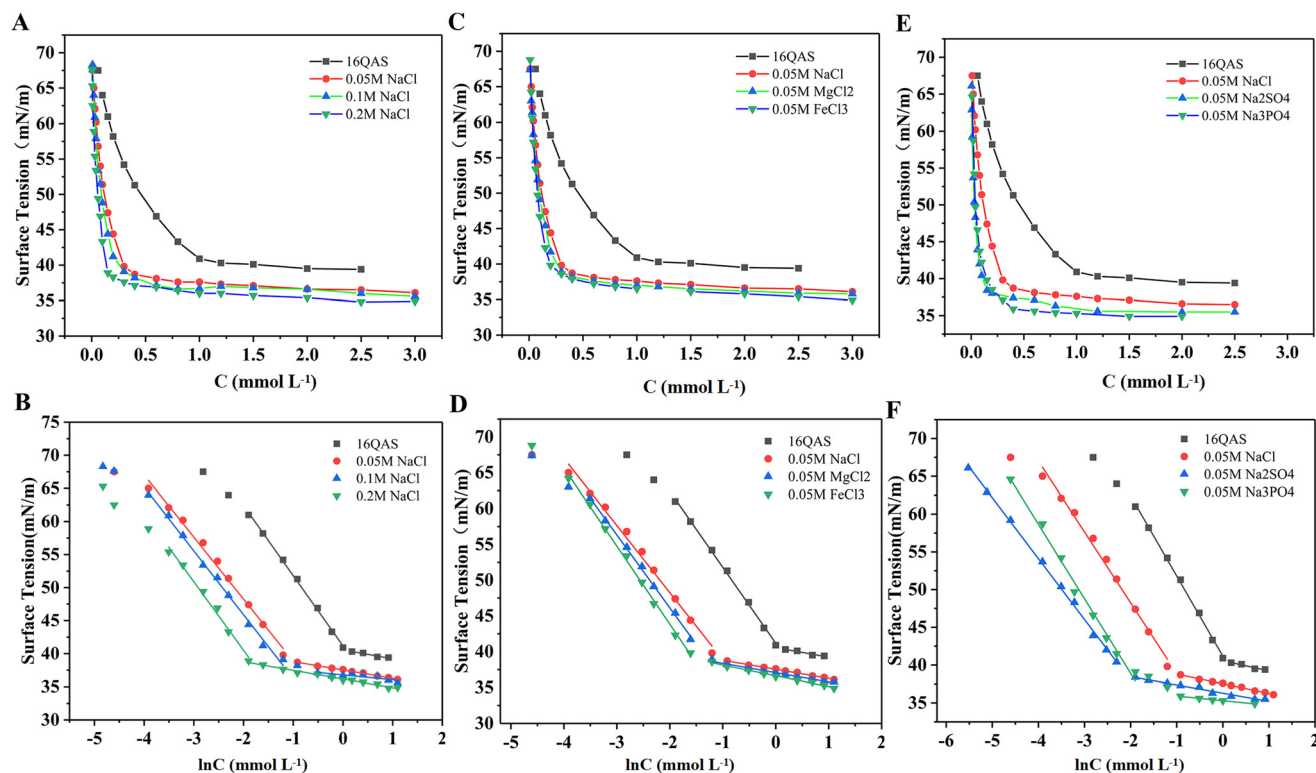

Fig. 5 Effect of electrolyte type and concentration on the surface tension of 16QAS. (A) and (B) The effect of NaCl concentration. (C) and (D) The effect of cation valence states at the same concentration. (E) and (F) The effect of counterions of different valence states at the same concentration.

equilibrium surface tensions ($\gamma_{eq.}$), aggregation number, or Krafft temperature.[32]

With 16QAS as a typical surfmer, the influence of electrolyte type and concentration on the surface tension curve of the surfactants was studied; the results are shown in Fig. 5. Furthermore, the interfacial adsorption parameters were calculated, and the results are listed in Table 2. Firstly, the surface tension curves of 16QAS in NaCl solutions of different concentrations were studied. Whereas the critical micelle concentration of 16QAS in pure water was 1.05 mmol L^{-1}, the CMC in solutions of 0.05, 0.1 and 0.2 mol L^{-1} NaCl were 0.37, 0.33 and 0.16 mmol L^{-1}, respectively. The lowest surface tension (γ_{cmc}) of 16QAS in pure water was 39.4 mN m^{-1}, and the γ_{cmc} values in 0.05 M, 0.1 M and 0.2 M NaCl solutions were 36.1, 35.6 and 34.9 mmol L^{-1}, respectively. The lower CMC values and lower surface tension indicate that the solution exhibited improved surface activity due to the introduction of the electrolytes. With increasing electrolyte concentration, the CMC value of the surfactant decreases gradually, and the minimum surface tension of the solution decreases to even lower values. This indicates that the introduction of electrolytes can promote the formation of cationic surfmer micelles.

Metal ions with different valence states were also used to study their effect on the surface tension curves. It is generally believed that the effect of electrolytes on the stacking of surfactant molecules and the formation of micelles is achieved through metal ion bridging, so it is necessary to study the influence of metal ions with different valence states. The surface tension curves of 16QAS in 0.05 mol L^{-1} solutions of NaCl, MgCl$_2$, and FeCl$_3$ were determined, and the results are shown in Fig. 5(C) and (D). Compared with the minimum surface tension of 39.4 mN m^{-1} and CMC of 1.05 mmol L^{-1}, all three types of electrolyte reduced the minimum surface tension of 16QAS and CMC to 36.1, 35.7 and 34.9 mN m^{-1}, and the CMC could be decreased to 0.37, 0.28 and 0.21 mmol L^{-1}, respectively. Moreover, as the valence state of the metal ions increased, the degree of reduction in the surface tension and critical micelle concentration increased, indicating that the higher the valence state of the metal ions, the more significant their bridging degree.

In order to further investigate the effect of anionic valence states on the surface tension of 16QAS, the surface tension curves of 16QAS in 0.05 mol L^{-1} solutions of NaCl, Na$_2$SO$_4$, and Na$_3$PO$_4$ were determined; the results are shown in Fig. 5(E) and (F). As shown in Table 2, as the anionic valence state increases, the minimum surface tension gradually decreases to 36.1, 35.5 and 34.9 mN m^{-1}. More significantly, the decrease in CMC is more pronounced, decreasing from 0.37 to 0.13 and 0.18 mmol L^{-1} when the anionic valence state changed from −1 to −3, which indicates that the electrolyte anions also have a significant impact on the interfacial packing of cationic surfactants, particularly affecting their critical micelle concentration.[33]

3.3 Solution micropolarity

It has long been recognized that surfactants can affect the spectral properties of dyes in solution. The absorption and fluorescence emission spectra of dye molecules are changed due to the complex interaction between surfactants and dye molecules. Based on the spectral changes of dye molecules, the assembly structure of surfactant solutions can be revealed through techniques such as pyrene fluorescence spectroscopy[24] and dye solubilization, which can be used to determine the critical micelle concentration of surfactants.[34] Methyl Orange (MO) is an example of an amphiphilic anionic azo dye that can interact with several cationic surfactants. Especially, the short wavelength absorption band of methyl orange, as induced by low concentrations of surfactant, has been used to infer the surfactant's assembly. MO probe molecules were dissolved in samples of the four polymerizable quaternary ammonium surfmers at different concentrations, and the UV-vis absorption spectra were recorded (Fig. 6). The absorption spectra indicated that the chain lengths of the surfmers have a dramatic influence on the absorption spectra of methyl orange. From Fig. 6(A)–(E), the maximum absorbance (λ_{max}) of MO in pure water was at 464 nm. According to the results of Engberts et al.,[35] the absorption band maximum (λ_{max}) for MO in water is at ca. 466 nm and at ca. 417 nm in ethanol, indicating that a more apolar environment leads to a substantial decrease in λ_{max}. When the surfactant concentration is lower than the CMC, the absorbance of free methyl orange at 464 nm in solution decreases, while a new absorption band appears at 375 nm with increasing concentration, which is attributed to the ion pair formed by the electrostatic interaction of 1 : 1 MO/surfactant. When the surfmer concentrations were further increased to values above the CMC, the maximum absorption of MO shifted to 416 nm, which indicates that methyl orange is incorporated into the micellar environment.

In order to study the effect of the length of the hydrophobic chain on the micellar environment, the absorption spectra of MO in several cationic surfactant solutions at 1 mmol L^{-1} were recorded, as shown in Fig. 6(F). The solution of MO in 12QAS showed a similar absorption profile to that in pure water, which indicated that 12QAS showed weak micelle formation capability due to its shorter hydrophobic chain length. MO in 14QAS

Table 2 The effect of electrolyte type and concentration on the interfacial adsorption parameters of 16QAS

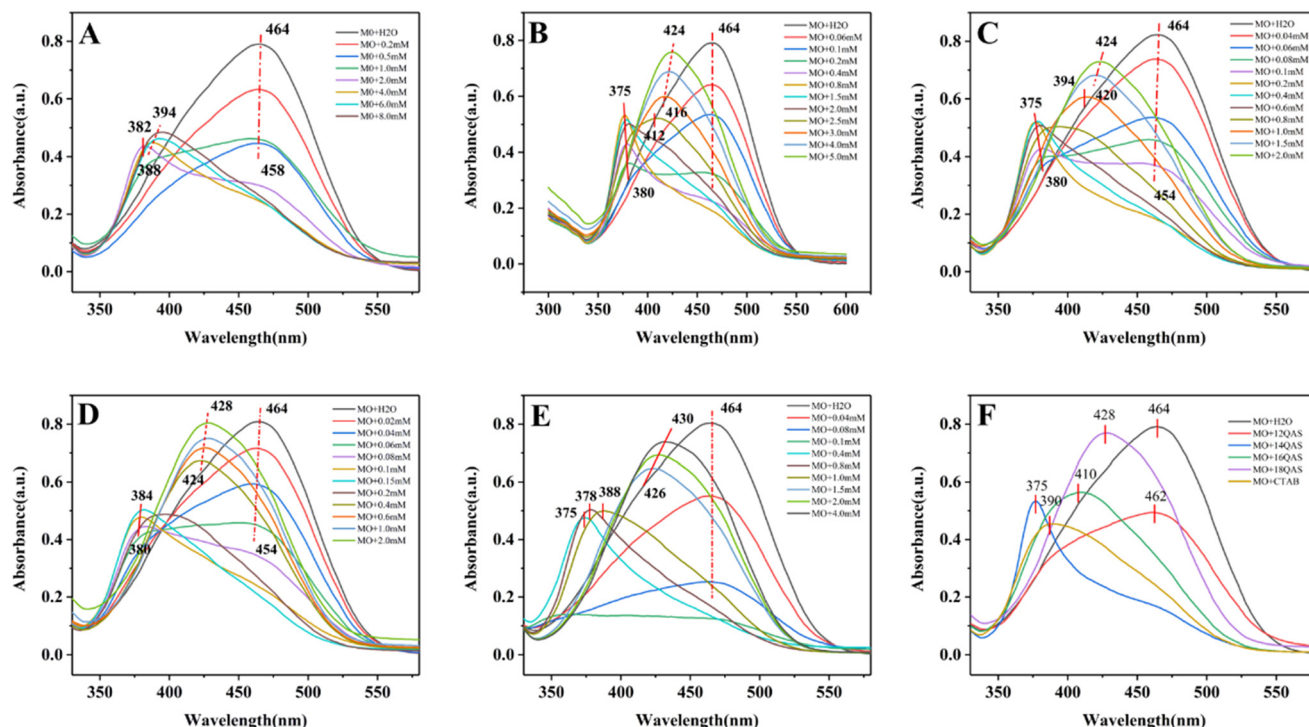| Solution	γ_{cmc}	CMC (mmol L^{-1})	Γ (μmol m^{-2})	A_{min} (Å^2)	pC$_{20}$
Pure water	39.4	1.05	2.14	77.48	1.019
0.05 M NaCl	36.1	0.37	1.90	87.66	2.399
0.1 M NaCl	35.6	0.32	1.95	85.20	2.647
0.2 M NaCl	34.9	0.16	2.09	79.33	3.108
0.05 M MgCl$_2$	35.7	0.28	2.06	80.64	2.576
0.05 M FeCl$_3$	34.9	0.21	2.20	75.40	2.747
0.05 M Na$_2$SO$_4$	35.5	0.13	1.63	102.00	3.740
0.05 M Na$_3$PO$_4$	34.9	0.18	1.99	83.38	3.326

Fig. 6 The microenvironment characterization of surfactant solutions of different concentrations with methyl orange as a probe. (A)–(E) The absorption spectra of methyl orange in different surfactants (12QAS, 14QAS, 16QAS, 18QAS, and CTAB). (F) The absorption spectra of methyl orange in the same concentration of surfactant solution. Concentration: 1.0 mmol L^{-1}.

solution at 1 mmol L^{-1} showed the strongest absorption at 375 nm, which implied that a complex aggregation of 14QAS and methyl orange occurred through electrostatic interactions. The MO in solutions of CTAB, 16QAS and 18QAS showed similar absorptions from 400 to 440 nm, which indicated that micellar structures had formed, and that the different vesicle structures with decreasing micro-polarity could contribute to the red-shift of absorption peaks. On the other hand, the CMC values shown in Fig. 6 reveal that the CMC decreases with hydrophobic chain length, with 12QAS > 14QAS > 16QAS > 18QAS, which is consistent with the CMC measured by the surface tension curves method.

3.4 *In vitro* antibacterial effect

Using the classical colony counting method, the antibacterial effects of several quaternary ammonium salts with different carbon chain lengths on *E. coli* and *S. aureus* were evaluated. The results are illustrated in Fig. 7. Fig. 7(A) and (B) show plates of *E. coli* and *S. aureus* treated with different quaternary ammonium surfmers under the same conditions. From the plate images, it can be observed that both *E. coli* and *S. aureus* have large numbers of colonies on the 12QAS plates, while the number of colonies on the 14QAS and 16QAS plates gradually decrease. This indicates that the antibacterial efficacy of the QAS surfmers can be enhanced with increasing carbon chain length.[17] This may be attributed

to the longer carbon chains having higher lipid solubility, which enables their penetration into the cell membrane and the cell, resulting in bacterial inactivation. Interestingly, for 18QAS, almost no colonies of *S. aureus* were observed on the agar plate, while the number of *E. coli* colonies increased. It is clear that 18QAS has a strong bactericidal effect on *S. aureus* but a weaker bactericidal effect on *E. coli*, which may be due to structural differences between Gram-positive and Gram-negative bacteria. Since the cell wall of Gram-positive bacteria is thicker, quaternary ammonium salts can penetrate more easily, disrupting cell membrane permeability and leading to leakage of intracellular contents.[36] Generally, there is no efficient antibacterial agent for all pathogenic microorganisms, and antibacterial agents have selectivity for microbial species.

In order to analyze the antibacterial performance of different samples more accurately, the colony-forming counting (CFU) method was used to analyze the antibacterial results, and the quantitative $\log_{10}$CFU results are shown in Fig. 7(C). With increasing hydrophobic tail length, the $\log_{10}$CFU reduction of QAS surfmers against *S. aureus* gradually increases, reaching a max of 4.23 for 18QAS. However, compared to 12QAS, the 14QAS and 16QAS surfmers show a greater reduction in $\log_{10}$CFU for *E. coli*, and 16QAS showed the best antibacterial performance (2.61 $\log_{10}$CFU). Strangely, 18QAS only achieved a reduction of 0.43 $\log_{10}$CFU for *E. coli*, which is consistent with the trend of bacterial colony growth on
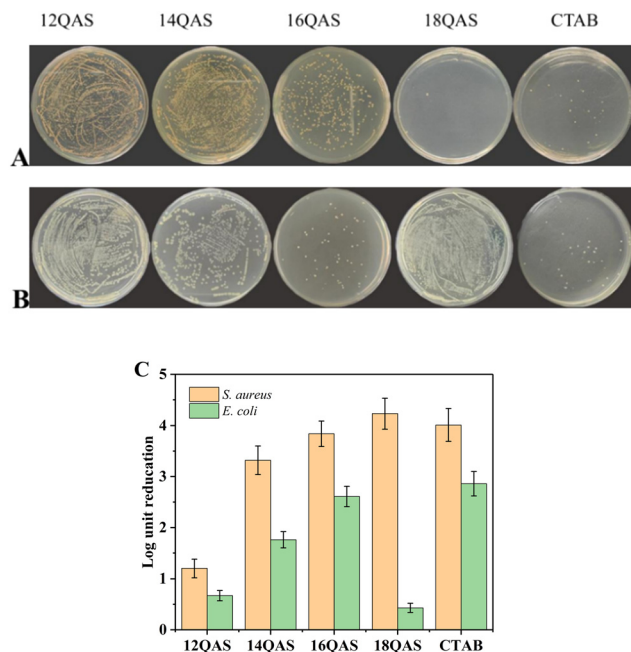
Table 3 MIC and MBC of amphiphilic QASs against *S. aureus* and *E. coli*

QASs	MIC (μmol L^{-1})		MBC (μmol L^{-1})	
	S. aureus	*E. coli*	*S. aureus*	*E. coli*
12QAS	3.75	125	15	125
14QAS	1.875	62.5	7.5	62.5
16QAS	<1.875	32.25	<7.5	32.25
18QAS	0.937	>1000	3.75	>1000
CTAB	<1.875	<32.25	<7.5	<32.25

Fig. 7 *In vitro* antibacterial activity. Plate images of *Staphylococcus aureus* (A) and *Escherichia coli* (B) treated with QASs. Bacteria were incubated with quaternary ammonium surfmers (5 μmol L^{-1}, *S. aureus*; 10 μmol L^{-1}, *E. coli*) and CTAB was used as a positive control for both *S. aureus* and *E. coli*. (C) Qualitative colony-forming unit chart of the inhibitory effects on the two types of bacteria treated with different QASs.

agar plates, as shown in Fig. 7(B). Additionally, 12QAS exhibits certain antibacterial activity against *S. aureus* and *E. coli*, with log$_{10}$CFU reduction rates of 1.2 and 0.67, respectively. This may be related to the quaternary ammonium structure, given that a large number of quaternary ammonium cationic surfactants have been shown to possess antimicrobial activity.[37]

3.5 MIC and MBC

In order to further compare the bacteria killing efficiency of polymerizable quaternary ammonium surfmers, the minimum inhibitory concentration (MIC) and minimum bactericidal concentration (MBC) were determined. Turbidity was used to identify bacterial growth, with no turbidity indicating an inhibitory effect on bacterial growth. The corresponding MIC and MBC values are listed in Table 3.

Except for 18QAS, the MIC values for the surfmer against *E. coli* are mainly concentrated at 32.25–125 μmol L^{-1}, and their MIC values against *S. aureus* are 1–4 μmol L^{-1}. Strangely, the 18QAS surfmer showed very low MIC and MBC against *S. aureus*, at 0.937 and 3.75 μmol L^{-1}, respectively, which demonstrated that the 18QAS surfmer exhibited a superior bactericidal and inhibitory efficiency compared with the other polymerizable quaternary ammonium surfmers. However, the 18QAS surfmer exhibited unusually low bactericidal and inhibitory efficiency against *E. coli*, at over 1000 μmol L^{-1}. For the

inhibition efficiency of *E. coli*, the 16QAS showed the best bactericidal and inhibitory efficiency, at concentrations of 32.25 and 32.25 μmol L^{-1}, respectively. Compared with the control sample CTAB, its efficiency was slightly weaker. These results agree with the conclusion from qualitative colony-forming unit protocols. On the other hand, each QAS surfmer has a higher MIC value against *E. coli* than against *S. aureus*. In our previous reports,[20,23,24,38] different amphiphilic cationic photosensitizers were synthesized and used to kill Gram-negative *P. aeruginosa* and Gram-positive *S. aureus* through an antibacterial photodynamic therapy process, and the results revealed higher antibacterial efficiencies against Gram-positive bacteria than against Gram-negative bacteria, which are consistent with our current results. In our previous research,[20,23,24,38] we explored the antibacterial mechanism using SEM and confocal fluorescence microscopy. The results showed that Gram-positive bacteria are killed more easily by amphiphilic cationic antibacterial agents due to differences in their cell wall and membrane structures. The specific mechanism may involve electrostatic binding, hydrophobic chain insertion into the cell membrane, or a combination of both processes. Therefore, for the current results, 16QAS shows the best effect on Gram-negative *E. coli*, while 18QAS is highly effective against Gram-positive *S. aureus* but ineffective against Gram-negative *E. coli*. This 'cross-advantage' targeting different bacterial strains is very interesting. However, the complexity of microbial structures makes it difficult to clearly elucidate this mechanism at present. We think that QAS has stronger antibacterial activity against Gram-positive bacteria, which may be related to differences in cell wall composition. Gram-positive bacterial cell walls contain more peptidoglycans and phosphates, but porous peptidoglycans make it easier for foreign molecules to enter. The double-layer structure of Gram-negative bacterial cell walls can more effectively prevent the entry of foreign molecules, thus requiring higher concentrations of QAS for sterilization.

4. Conclusion

In conclusion, four polymerizable quaternary ammonium surfmers with different hydrophobic chain lengths have been synthesized, characterized and used as bacterial inhibitory and killing agents. As the length of the

hydrophobic chain increases, the minimum surface tension of these polymerizable quaternary ammonium surfmers gradually increases, while CMC gradually decreases, resulting in improved efficiency in reducing surface tension. On the other hand, not only does the electrolyte concentration increase the interfacial adsorption activity of surfmers, but the electrolyte composition, such as cation and anion valence states, also greatly enhances the surface activity reduction efficiency of these QAS surfmers. The 18QAS surfmer showed very low MIC and MBC against *S. aureus*, at 0.937 and 3.75 μmol L^{-1}, respectively, with an efficiency of 4.23 log CFU against *S. aureus*. 16QAS showed superior killing efficiency of 2.61 log CFU against *E. coli* at concentrations of 32.25 μmol L^{-1}. The introduction of the acrylate polymerizable group to the amphiphilic quaternary ammonium provides infinite possibilities for polymerizable cationic functionalized surfaces. These results provide ideas for the design of long-term antibacterial surfaces and implant material surfaces, thereby providing a reference for the interface design of biological functional materials.

Author contributions

Cailing Li: data curation, methodology, writing, review & editing. Jinlu Zhong: data curation, investigation. Yanan Weng: methodology, investigation. Sensen Xie: conceptualization, methodology, review. Shuang Li: microbacterial data curation. Dinghua Yu: supervision, data curation, project administration, funding acquisition.

Conflicts of interest

The authors declare that they have no known competing financial interests or personal relationships that could have appeared to influence the work reported in this paper.

Data availability

The authors confirm that the data supporting the findings of this study are available within the article.

Acknowledgements

References

1 Q. Su, Y. Xue, C. Wang, Q. Zhou, Y. Zhao, J. Su and B. Zhu, *Bioact. Mater.*, 2025, **53**, 114–140.

2 S. W. M. A. Ishantha Senevirathne, J. Hasan, A. Mathew, A. Jaggessar and P. K. D. V. Yarlagadda, *ACS Appl. Bio Mater.*, 2021, **4**, 7626–7642.

3 C. Zhou and Y. Wang, *Curr. Opin. Colloid Interface Sci.*, 2020, **45**, 28–43.

4 E. Obłąk, A. Piecuch, J. Rewak-Soroczyńska and E. Paluch, *Appl. Microbiol. Biotechnol.*, 2019, **103**, 625–632.

5 Y. Xue, Z. Zhao, W. Huang, Z. Qiu, X. Li, Y. Zhao, C. Wang, R. Cui, S. Shen, H. Tian, L. Fang, R. Zhou and B. Zhu, *J. Mater. Chem. B*, 2023, **11**, 7750–7765.

6 B. Zhang, D. Lu, D. B. R. Wang, Z. Y. Kok, M. B. Chan-Park and H. Duan, *Adv. Funct. Mater.*, 2024, **34**, 2407869.

7 Z. Deng, R. Zhang, J. Gong, Z. Zhang, L. Zhang, Z. Qiu, P. Alam, J. Zhang, Y. Liu, Y. Li, Z. Zhao and B. Z. Tang, *JACS Au*, 2025, **5**, 675–683.

8 X. Wang, Y. Liu, T. Wu, B. Gu, H. Sun, H. He, H. Gong and H. Zhu, *Bioorg. Chem.*, 2023, **134**, 106448.

9 D. Zhou, D. Wang, M. Cao, Y. Chen, Z. Liu, C. Wu, H. Xu, S. Wang and Y. Wang, *ACS Appl. Mater. Interfaces*, 2016, **8**, 30811–30823.

10 Y. Shen, S. Li, R. Qi, C. Wu, M. Yang, J. Wang, Z. Cai, K. Liu, J. Yue, B. Guan, Y. Han, S. Wang and Y. Wang, *Angew. Chem., Int. Ed.*, 2022, **61**, e202110938.

11 M. Summers and J. Eastoe, *Adv. Colloid Interface Sci.*, 2003, **100–102**, 137–152.

12 D. Hodyna, V. Kovalishyn, S. Rogalsky, V. Blagodatnyi, K. Petko and L. Metelytsia, *Chem. Biol. Drug Des.*, 2016, **88**, 422–433.

13 A. Cornellas, L. Perez, F. Comelles, I. Ribosa, A. Manresa and M. T. Garcia, *J. Colloid Interface Sci.*, 2011, **355**, 164–171.

14 J. Pernak, K. Sobaszkiewicz and I. Mirska, *Green Chem.*, 2003, **5**, 52–56.

15 B. Gao, Y. Yu and L. Jiang, *Colloids Surf., A*, 2007, **293**, 210–216.

16 R. Mancuso, R. Amuso, B. Armentano, G. Grasso, V. Rago, A. R. Cappello, F. Galiano, A. Figoli, G. De Luca, J. Hoinkis and B. Gabriele, *ChemPlusChem.*, 2017, **82**, 1235–1244.

17 M. T. Garcia, I. Ribosa, L. Perez, A. Manresa and F. Comelles, *Colloids Surf., B*, 2014, **123**, 318–325.

18 J. Hoque, S. Gonuguntla, V. Yarlagadda, V. K. Aswal and J. Haldar, *Phys. Chem. Chem. Phys.*, 2014, **16**, 11279–11288.

19 C. Bonnet, P. Guillet, F. Mahler, S. Igonet, S. Keller, A. Jawhari and G. Durand, *Eur. J. Org. Chem.*, 2020, **33**, 5340–5349.

20 X. Gu, H. Yuan, C. Li, L. Xu, S. Li and D. Yu, *Colloids Surf., B*, 2024, **233**, 113657.

21 Y. Cao, Z. Yang, J. Ou, L. Jiang, G. Chu, Y. Wang and S. Chen, *Prog. Org. Coat.*, 2023, **175**, 107369.

22 F. Hu, Y. Liu, J. Lin, W. Wang, D. Yu and S. Li, *Colloids Surf., B*, 2021, **200**, 111602.

23 H. Zhang, L. Xu, X. Gu, D. Yu and S. Li, *RSC Adv.*, 2023, **13**, 239–250.

24 J. Zhao, L. Xu, H. Zhang, Y. Zhuo, Y. Weng, S. Li and D. Yu, *Colloids Surf., B*, 2021, **207**, 111974.

25 P. Parvekar, J. Palaskar, S. Metgud, R. Maria and S. Dutta, *Biomater. Invest. Dent.*, 2020, **7**, 105–109.

26 R. Tang, A. Muhammad, J. Yang and J. Nie, *Polym. Adv. Technol.*, 2014, **25**, 651–656.

27 L. Martínez-Balbuena, A. Arteaga-Jiménez, E. Hernández-Zapata and C. Márquez-Beltrán, *Adv. Colloid Interface Sci.*, 2017, **247**, 178–184.

28 M. J. Vold, *Langmuir*, 1992, **8**, 1082–1085.

29 A. Rodríguez, M. M. Graciani, M. Muñoz, I. Robina and M. L. Moyá, *Langmuir*, 2016, **22**, 9519–9525.

30 M. Abo-Riya, A. H. Tantawy and W. El-Dougdoug, *J. Mol. Liq.*, 2016, **221**, 642–650.

31 Z. Derikvand, A. Rezaei, R. Parsaei, M. Riazi and F. Torabi, *Colloids Surf., A*, 2020, **587**, 124327.

32 J. C. Roy, M. N. Islam and G. Aktaruzzaman, *J. Surfactants Deterg.*, 2014, **17**, 231–242.

33 M. Sammalkorpi, M. Karttunen and M. Haataja, *J. Phys. Chem. B*, 2009, **113**, 5863–5870.

34 M. Bielska, A. Sobczyńska and K. Prochaska, *Dyes Pigm.*, 2009, **80**, 201–205.

35 J. M. Kuiper, R. T. Buwalda, R. Hulst and J. B. F. N. Engberts, *Langmuir*, 2001, **17**, 5216–5224.

36 J. Hoque, M. M. Konai, S. Samaddar, S. Gonuguntala, G. B. Manjunath, C. Ghosh and J. Haldar, *Chem. Commun.*, 2015, **51**, 13670–13673.

37 J. Hoque, P. Akkapeddi, V. Yarlagadda, D. S. S. M. Uppu, P. Kumar and J. Haldar, *Langmuir*, 2012, **28**, 12225–12234.

38 X. Gu, L. Xu, H. Yuan, C. Li, J. Zhao, S. Li and D. Yu, *RSC Adv.*, 2023, **13**, 11782–11793.